Vibrational Predissociation of *p*-Difluorobenzene·Ar Studied by Mass-Analyzed Threshold Ionization Spectroscopy

Gerhard Lembach and Bernhard Brutschy*

Institut für Physikalische und Theoretische Chemie, J. W. Goethe Universität Frankfurt, Marie-Curie-Strasse 11, 60439 Frankfurt/Main, Germany

Received: February 4, 1998; In Final Form: May 7, 1998

Mass-analyzed threshold ionization (MATI) spectroscopy has already proven to be a powerful method for the study of the fragmentation energetics and dynamics of molecular clusters in the cationic state. In this study, its application was extended to the investigation of the vibrationally induced predissociation (VP) of van der Waals (vdW) clusters in vibronically excited states (S_1). To verify the feasibility of MATI spectroscopy for studies of this type, the *p*-difluorobenzene·Ar_1 (*p*-DFB·Ar_1) complex has been chosen as a model system. The state and mass selectivity of MATI spectroscopy promise to give useful supplementary information about the VP process, which would be difficult or even impossible to obtain by conventional methods such as fluorescence spectroscopy and time-resolved resonant two-photon ionization spectroscopy. (Butz, K. W.; et al. *J. Phys. Chem.* **1986**, *90*, 3533. Jacobson, B. A.; et al. *J. Chem. Phys.* **1988**, *89*, 5624.) In accordance with the pioneering studies of Parmenter et al., who investigated the predissociation of the vibronically excited *p*-DFB·Ar_1 complex very extensively by means of UV fluorescence spectroscopy, (Butz et al., 1986), the MATI spectra give evidence for the strong mode selectivity of the VP process. However, from the MATI results, evidence is given that additional fragmentation channels appear, which have not been observed in the fluorescence spectra. On the basis of the fragmentation thresholds observed in the MATI spectra, we also deduced upper and lower limits for the dissociation energies of the complex in the S_0, S_1, and ionic ground state, which differ significantly from those determined by Parmenter et al.

1. Introduction

In recent years, zero kinetic energy photoelectron spectroscopy (ZEKE-PES), contrived by Müller-Dethlefs et al.,[3,4] and particularly mass-analyzed threshold ionization (MATI) spectroscopy, developed by Zhu and Johnson,[5] have grown into very powerful tools for cluster spectroscopy, allowing the detailed study of the ionic state of weakly bound van der Waals clusters. The simplest type of these clusters may be viewed as microsolvates, consisting of a chromophore surrounded by a certain number of solvent atoms or molecules. Aside from the dependence of the chromophore's ionization energy from the number of solvent molecules attached to it, the intermolecular interactions between an ion and such a well-defined molecular environment are of great interest, for a basic understanding both of the reactivity of solvated species and of the intermolecular energy transfer involved. The solvated chromophore, which is, in general, vibrationally excited after its photoionization, is subject to different relaxation processes. Up to now, most studies have focused on van der Waals fragmentation, intermolecular charge transfer, and chemical substitution reactions.[6,7] The main issue of studying the reactivity of this type of clusters on a molecular level is to derive information about the physical and chemical properties of microsolvated species and their structure with the prospect of a better understanding of ion chemistry in the condensed phase. Hitherto, the focal point of most MATI and recently also of some ZEKE-PES studies has been put on the fragmentation behavior of van der Waals complexes in the vibrationally excited cationic state.[8−14] However, ZEKE spectroscopy is not only suitable for the spectroscopic characterization of the ionic state of molecules and molecular complexes but also allows important data to be derived about the intermolecular relaxation in vdW complexes and particularly of the predissociation of a vibronically excited complex. This was first demonstrated by Knee et al.[15−18] Nevertheless, it is often very difficult to derive unambiguous information about the different relaxation channels by the ZEKE-PES method. This is especially true if the product states are not well-resolved or spectroscopically distinct from the parent complex. MATI spectroscopy, however, is based on the detection of so-called *threshold ions* in contrast to the photoelectrons, detected by ZEKE spectroscopy. As has been shown in several publications, these threshold ions stem from long-lived *Rydberg states*, also called ZEKE states, which may survive inter- as well as intramolecular dissociation of their ionic core.[8−14,19] In addition to the observation of a reaction (e.g., fragmentation) in the vibrationally excited ionic state of a complex, also the predissociation of a neutral vibronically excited complex can be detected. This was first shown by our group for the fluorobenzene·Ar_1 cluster, for which we could establish the vibrationally induced predissociation of the complex after the excitation of the $6b^1$ level (*Wilson notation*, ref 20; the vibrational mode ν_{6b} is equivalent to the vibrational mode ν_{29} in the *Mulliken notation*, ref 21) in the S_1 state.[22] One essential point for the observation of the predissociation of a complex by MATI or ZEKE spectroscopy is that one of the fragments remains in a vibronically excited state, from which it can then be transferred into a long-lived Rydberg state by a second laser pulse. The decisive advantage of MATI compared to other spectroscopic methods (e.g., fluorescence spectroscopy)

S1089-5639(98)01004-4 CCC: $15.00
Published on Web 07/03/1998

is that each of the different decay channels can be observed mass selectively.

To verify the versatility of MATI spectroscopy with respect to the investigation of the VP process of vibronically excited complexes, we have chosen the *p*-difluorbenzene·Ar_1 cluster (1,4-$C_6H_4F_2$·Ar_1, *p*-DFB·Ar_1) for our first study. As demonstrated in the pioneering work of Parmenter et al., this simple vdW system represents an ideal model on which to study intermolecular energy transfer. Owing to numerous absorption and fluorescence measurements, most $S_1 \leftarrow S_0$ transitions of *p*-difluorobenzene are well-known.[23−26] The cationic states have been investigated with conventional photoelectron spectroscopy[27,28] and recently with ZEKE spectroscopy by Müller-Dethlefs et al.[29,30] Parmenter and co-workers studied the predissociation of *p*-DFB·Ar_1 in various vibrationally excited states of the S_1 by means of laser-induced UV fluorescence emission spectroscopy.[1,31,32] On the basis of the dispersed fluorescence spectra, which they recorded after the excitation of a distinct vibration in the S_1 state of the complex, they determined the relative population of the final states of the fragment *p*-DFB, produced by VP. From their analysis, they found evidence that this cluster predissociates nonstatistically. Assuming equal fluorescence quantum yields and equal fluorescence rate constants ($k_f = 10^8$ s^{-1}, ref 33) for all excited states of the complex as well as for the final states of the fragment, they could determine rate constants for the different fragmentation channels (for more details, see section 4.2.2 of this article). On the basis of these measurements, they also made a rough estimation for the van der Waals binding energy of the complex. In their first study, they claimed that the fragmentation threshold lies between 378 and 410 cm^{-1},[1] which they later corrected to 190 and 240 cm^{-1}, respectively.[31,32]

Rice et al. studied the predissociation of *p*-DFB·Ar by means of time-resolved two-color resonant two-photon (2C-R2PI) pump−probe spectroscopy.[2] Analogous to the fluorescence experiments, they excited various vibrational levels in the S_1 state of the complex. Subsequently, the vibronically excited clusters were ionized by a delayed laser pulse, and the ion current was finally analyzed by means of a mass spectrometer. By varying the delay of the ionizing laser relative to the excitation pulse, Rice and co-workers could observe the decay of the originally populated vibrational state. However, owing to the fact that they only detected the ionized complex, they could only determine the total rate constant for the predissociation of the complex in a certain, previously excited vibronic state. Hence no information about the final states of the monomer emerged from these studies.

2. Experiment

An in depth description of the experimental setup has already been given elsewhere.[22] Briefly, a pulsed supersonic molecular beam is produced by expanding the *p*-DFB vapor seeded in 4−5 bar of helium, argon, or a helium/argon mixture through a 300 μm nozzle (General Valve VAC-1250). After passing a 1.9 mm skimmer, the molecular beam enters the ionization chamber where it is intersected by two counterpropagating laser beams. The latter are generated by two frequency-doubled dye lasers (Lambda Physik FL 2002), which are synchronously pumped by an excimer laser (Lambda Physik LPX 200). The frequency-doubling crystals are angle-tuned by an autotracking system (Radiant Dyes SCANTRACK). The ionic molecules or clusters, produced under field-free conditions by two-color resonant two-photon ionization, are analyzed by means of a reflectron time-of-flight mass spectrometer mounted perpendicular to the axis of the molecular beam as well as both laser beams. The neutral *Rydberg molecules* are spatially separated from the simultaneously produced direct ions by applying a weak electric separation field some 100 ns after the laser pulses. Since the S_1 vibrational states of *p*-DFB are located approximately halfway to the ionization limit, it is possible that the "ionizing" laser accidentally hits a $S_1 \leftarrow S_0$ transition, which would result in the production of additional direct ions, mainly owing to a one-color ionization process, resulting in a dramatic increase of the ion density. This again could lead to a falsification of the recorded MATI spectra by the appearance of artificial peaks. To suppress these unwanted S_1 resonances in the MATI spectra, the separation field (1.5−1.9 V/cm) had to be increased substantially compared to the values in our former MATI studies.[12,13,22] To optimize the production of 1:1 clusters while reducing the portion of higher clusters and simultaneously minimize these unwanted S_1 resonances, different He/Ar mixtures for the expansion gas have been tested. By increasing the He portion, the production of higher *p*-DFB·Ar_n complexes could be reduced significantly. However, the suppression of one-color ions was more difficult, because the amount of free *p*-DFB molecules increases correspondingly under these conditions. Thus most cluster spectra have been recorded by expanding *p*-DFB with pure Ar. After a separation time of 10−20 μs a pulsed electric field (extraction field) of 2000 V/cm induces the field ionization of the remaining high-lying, long-lived Rydberg states. Since the directly produced ions and the ions originating from Rydberg states are spatially separated, they are on different potentials and hence are accelerated to different kinetic energies. Owing to this difference in energies, the directly produced ions can be suppressed easily by the use of a high-pass energy filter. Either this can be a pulsed reflector field in the usually field-free drift region, or one can use the ion mirror of the RETOF mass spectrometer as an energy analyzer.[22] The ion current is measured by a detector consisting of a set of two multichannel plates. The resulting signal is then further amplified before it is passed into a CAMAC-based transient recorder (LeCroy TR8828C). The recorded mass spectra are averaged and analyzed by a personal computer.

The threshold ion spectra are obtained by tuning the excitation laser to a particular S_1 intermediate state (fingerprint state) and scanning the ionizing laser in the region of the cationic states of the molecules or clusters investigated. The calibration of the dye lasers was achieved by means of a wavemeter (ATOS, Lambdameter LM 007). The quoted ionization potentials are accurate to within ± 5 cm^{-1}, while the vibrational frequencies are accurate to within ± 2 cm^{-1}.

3. Results

3.1. Two-Color Resonant Two-Photon Ionization (2C-R2PI) Spectra. Figure 1 shows the 2C−R2PI spectra of *p*-DFB (upper trace) and of the *p*-DFB·Ar_1 complex (lower trace), measured by scanning the excitation laser, while keeping the wavelength of the ionization laser fixed. Since the excitation energies of the vibrationless S_1 states of *p*-DFB and *p*-DFB·Ar_1 are lower than half the ionization energy, the ions produced via the $S_1 0^0$ bands are only due to two-color ionization. By exciting higher lying vibrational levels, the ions can also be produced by the excitation laser alone, i.e., by one-color R2PI. Thus the relative intensities of the $S_1 0^0$ bands, compared to the remaining vibrational bands in the S_1, do not reflect the corresponding *Franck−Condon* (*FC*) factors. The transition $S_1(^1B_2) \leftarrow S_0(^1A_1)$ in *p*-DFB·Ar_1 is electronic dipole allowed, and the transition moment is directed along the short in-plane axis of *p*-DFB (see inset in Figure 1).[34]

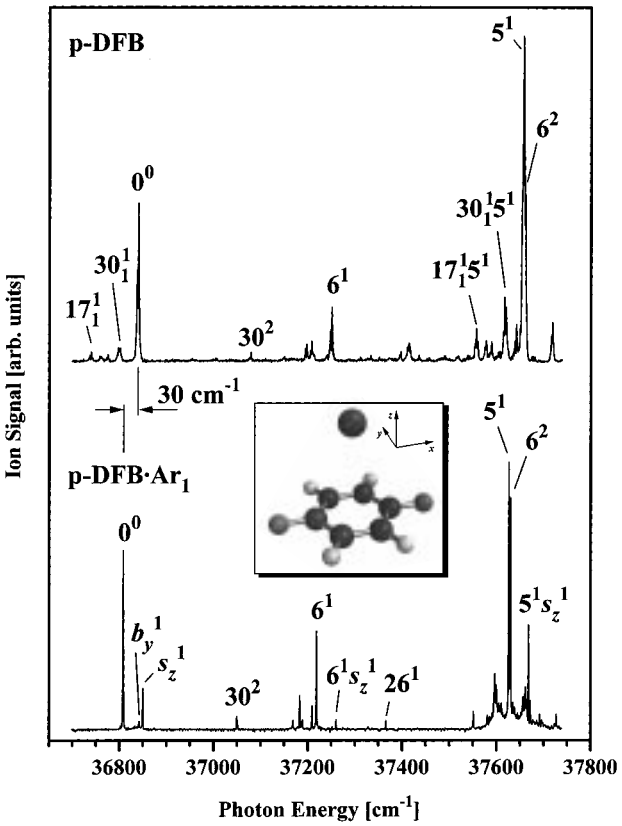

Figure 1. 2C-R2PI spectra of *p*-DFB (upper trace) and *p*-DFB·Ar$_1$ (lower trace). The inset in the lower part shows the configuration of the *p*-DFB·Ar$_1$ complex and the used coordinate system. The representation is based on data from ab initio calculations[39] and rotationally resolved UV spectroscopy.[40]

The vibrationless transition $S_1 \leftarrow S_0$ 0_0^0 in *p*-DFB·Ar$_1$ (36 808.0 cm^{-1}) is red-shifted relative to that of the *p*-DFB monomer (36 838.6 cm^{-1}) by about 30 cm^{-1}. The intermolecular stretching mode s_z appears 42 cm^{-1} above the 0_0^0 transition. It is also observed in combination with the intramolecular vibrations ν_5 and ν_6 of the chromophore (to be consistent with former publications of other authors, in this paper, the vibrations are denoted according to the Mulliken notation; ref 21). Provided that the Ar-atom is located on the C_{2v}-symmetry axis in the S_1 as well as in the cationic state, both van der Waals bending vibrations b_x and b_y, respectively, are not Franck−Condon active (symmetries: b_1 and b_2).[34] Owing to a strong coupling of electronic and vibrational degrees of freedom, the excitation of the bending vibration along the short in-plane axis of *p*-DFB (b_y) is vibronically allowed and is observed with a vibrational energy of 33.9 cm^{-1}.[34] In the case of the *p*-DFB monomer, the rotational contours of the bands 5^1 and 6^2 overlap, representing a mild *Fermi resonance* according to Parmenter. To optimize the signal-to-noise ratio, the excitation for MATI spectra of the monomer, discussed in the following, was performed via the *R*-branch of these bands.

3.2. Threshold Ion Spectra of p-Difluorobenzene. Even though the *p*-DFB monomer has already been investigated very extensively with the ZEKE-PES method by Reiser et al.,[30] the MATI spectra of the monomer play an important role in the interpretation of the predissociation spectra of *p*-DFB·Ar$_1$ measured with MATI. For this reason, the MATI spectra of the monomer, recorded after the excitation of different intermediate states, are presented here briefly. Most important are the spectra recorded via the vibrationless $S_1 0^0$ and the vibrationally excited $S_1 6^1$ intermediate states. Additional spectra

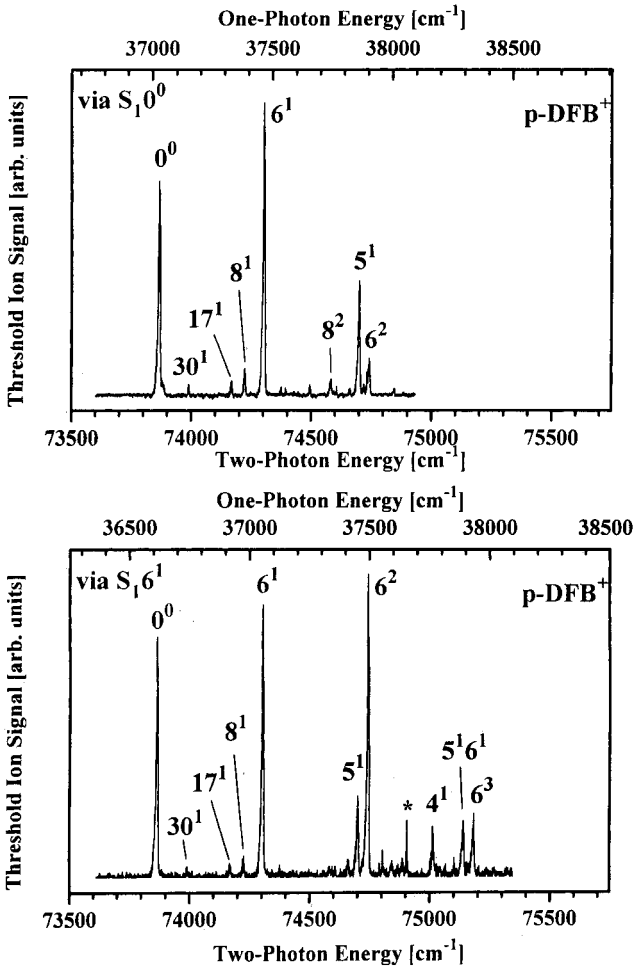

Figure 2. Threshold ion spectra of *p*-DFB$^+$, recorded via the vibrationless intermediate state $S_1 0^0$ (upper trace) and the vibrationally excited $S_1 6^1$ state (lower trace). The band marked by an asterisk is due to a S_1 resonance.

were recorded after the excitation of the levels 5^1 and 6^2. To simplify the comparison between bands in the spectra of the monomer and the *p*-DFB·Ar cluster, the energy values on the upper axis in the diagrams for the spectra recorded via the $S_1 0^0$ and the $S_1 6^1$ intermediate states (Figure 2) represent the one-photon-energy of the ionizing laser, while the total energy of the two-photon transition is given on the lower axis.

The threshold ion spectrum of *p*-DFB recorded via the vibrationless $S_1 0^0$ intermediate state is shown in Figure 2 (upper part). Apart from the 0_0^0 transition into the cationic ground state, the totally symmetric vibrational modes ν_6 (439 cm^{-1}) and ν_5 (836 cm^{-1}) dominate the spectrum. Also the first overtone of mode ν_6 (879 cm^{-1}) still lies within the investigated region. Besides these, also some nontotally symmetric modes such as the ν_{30} (126.5 cm^{-1}), ν_{17} (303 cm^{-1}), and ν_8 (359 cm^{-1}) are observed, but with significantly lower intensities. The width of the bands amounts to about 10 cm^{-1} (*full width at half-maximum, fwhm*). Compared to the spectrum from the ZEKE-PES studies of Reiser et al., the relative intensity of the 0_0^0 transition appears much too low. The reason for this discrepancy is still unclear. One possible explanation can be derived from the fact that the lifetime of Rydberg states is affected by the ionic background. Held et al. demonstrated that the reduction of the ZEKE-/MATI-signal due to static electric fields can be at least partly compensated by an increased ion density, which supports the mixing of different m_l states and results in an increased lifetime of the Rydberg states.[35] In 2C−R2PI

experiments via the $S_1 0^0$ state of *p*-DFB, no ions are produced below the adiabatic ionization energy, which could support the m_l mixing. Since the separation time in MATI experiments exceeds that of ZEKE-PES measurements significantly, more Rydberg states will therefore decay before they are detected by pulsed field ionization.

From the position of the 0° band in the MATI spectrum one obtains a field-corrected adiabatic ionization energy (*AIE*) for free *p*-DFB of 73 871 cm^{-1} ($\Delta E = 4.0\ (F(V/cm))^{1/2}\ cm^{-1}$; see ref 36), which is in good agreement with the value obtained by Reiser et al. (73 872 cm^{-1}).[30] In former studies, the *AIE* was determined to be 73 888 cm^{-1} by means of photoelectron time-of-flight measurements[27] and 73 871 cm^{-1} from an extrapolation of the Rydberg series.[37]

After excitation of the 6^1 level in the S_1 intermediate state, one observes, in accordance with the propensity rule, a pronounced progression of the vibrational mode ν_6 in the spectrum of the cationic state (lower part of Figure 2) corresponding to vibrations with up to three quanta. Most striking is the shift of the *Franck−Condon maximum* in this progression to the 6_1^2 transition, which has also been observed in the corresponding ZEKE[30] and time-of-flight photoelectron spectra.[27] The extremely sharp band marked by an asterisk is due to direct ionization via the $5^1/6^2$ Fermi resonance of the S_1 state. Its appearance indicates that the directly produced ions could not be totally suppressed. It may be mainly attributed to the unwanted one-color ionization due to the second, relatively intense laser ("ionizing laser"). But since the two laser pulses do overlap in time and the simultaneous absorption of a photon of each laser beam also induces ionization, part of the intensity may also be attributed to 2C-R2PI. Fortunately, this type of bands can be easily distinguished from the "real" MATI bands owing to its very sharp contour, which is typical for R2PI resonances in the S_1.

The threshold ion spectra recorded via the $S_1 5^1$ and $S_1 6^2$ intermediate states are shown in Figure 3. In both cases, the bands of the vibration ν_6 as well as some of its overtones dominate the spectra. Sekreta et al. attributed the strong excitation of the 6^1 level in the cation, following the excitation of the $S_1 5^1$ intermediate state, to the Fermi resonance between the 5^1 and the 6^2 levels in the S_1 state, which are only separated by about 3 cm^{-1} (see Figure 1).

Even though Reiser et al. did not record any ZEKE spectra via the $S_1 5^1$ and the $S_1 6^2$ intermediate states, from their work, most bands in the MATI spectra could be assigned very easily, with two important exceptions. In the spectrum recorded after excitation of the $S_1 5^1$, one relatively strong band appears between the ionic vibrational levels 5^1 and 6^2 at 855 cm^{-1}. The only fundamental mode in the cation observed by Reiser et al. close to this value is the mode ν_{28} (859 cm^{-1}). But since the primarily excited mode in the S_1 and the cationic mode ν_{28} are of different symmetry (a_g and b_{3u}, respectively), this assignment is very unlikely. However, an assignment to the combination band $17^2 30^2$ (860 cm^{-1}) or the first overtone of the vibrational mode ν_{27} (430 cm^{-1}) would be symmetry-allowed.

The spectrum recorded via the $S_1 6^2$ intermediate state again exhibits a progression of the vibrational mode ν_6. In the case where the 6^1 level is excited in the S_1, the most intense transition in the progression in the cation corresponds to $\Delta v = +1$. A similar propensity is observed for the $S_1 6^2$ intermediate state, since the 6^3 band in the cation is stronger in intensity than the bands 6^1 and 6^2. One remarkable feature in this spectrum is the appearance of a weak band (marked by *x*), 22 cm^{-1} above the vibrationless cationic ground state. The origin of this band could not be assigned. For an intramolecular mode of *p*-DFB, the excitation energy is much too low. In addition, no other MATI spectrum of the monomer exhibits a band corresponding to a similar low frequency. Since MATI spectroscopy is a mass-selective method, the contribution of different isotopomers of *p*-DFB exhibiting an isotopic shift of the 0^0 band can also be excluded. Further, it also cannot be caused by a not wholly suppressed S_1 resonance, since the photon energy of the ionizing laser lies still below the $S_1 0^0$ state. A similar band is observed above the 6^1 level, likewise with a distance of 22 cm^{-1}. Obviously the *x* mode also appears in combination with the vibrational mode ν_6. This would indicate that it is a vibrational mode of the ionized *p*-DFB monomer. However, the actual origin of the *x* bands is still unclear.

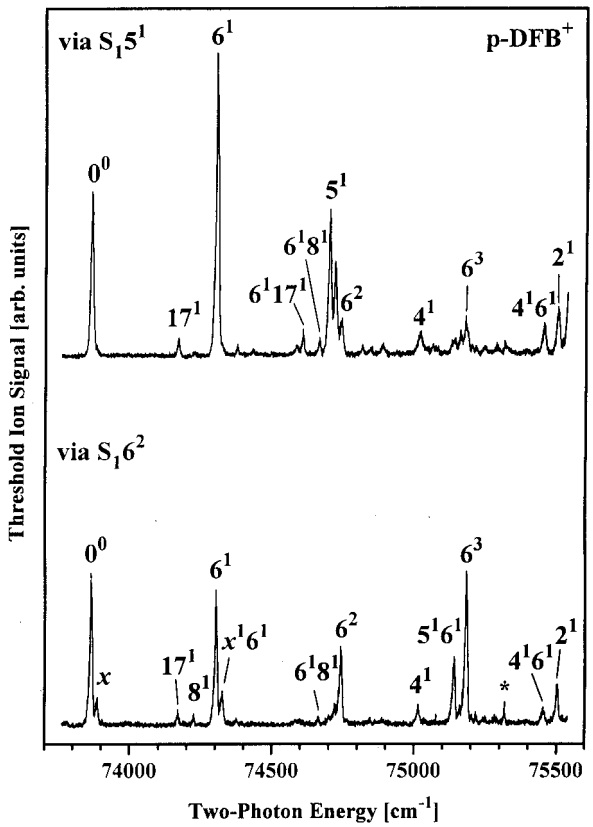

Figure 3. Threshold ion spectra of *p*-DFB$^+$, recorded via the vibrationally excited states $S_1 5^1$ (upper trace) and $S_1 6^2$ (lower trace). The band marked by an asterisk is due to a strong S_1 resonance. The band *x* (22 cm^{-1}) could not be assigned.

3.3. Threshold ion Spectra of the *p*-Difluorobenzene·Ar$_1$ Complex. Analogous to the *p*-DFB monomer measurements, the threshold ion spectra of the *p*-DFB·Ar$_1$ complex were recorded after excitation of the vibrationless band origin 0^0 as well as the intramolecular vibrations ν_5, ν_6, and $2\nu_6$ of *p*-DFB in the S_1 state of the complex. In addition, MATI spectra were recorded after excitation of the intermolecular stretching vibration s_z in the S_1 state. A series of measurements with different He/Ar mixtures as the carrier gas were carried out, trying both to optimize the yield of *p*-DFB·Ar$_1$ complexes in the molecular beam and to minimize the undesired appearance of S_1 resonances in the MATI spectra. Except for stronger S_1 resonances in the case where the expansion gas contains a high portion of He, the recorded spectra do not differ significantly. The MATI spectra, presented in the following for the intermediate states $S_1 0^0$, $S_1 s_z^1$, and $S_1 6^1$, were recorded by seeding *p*-DFB in pure

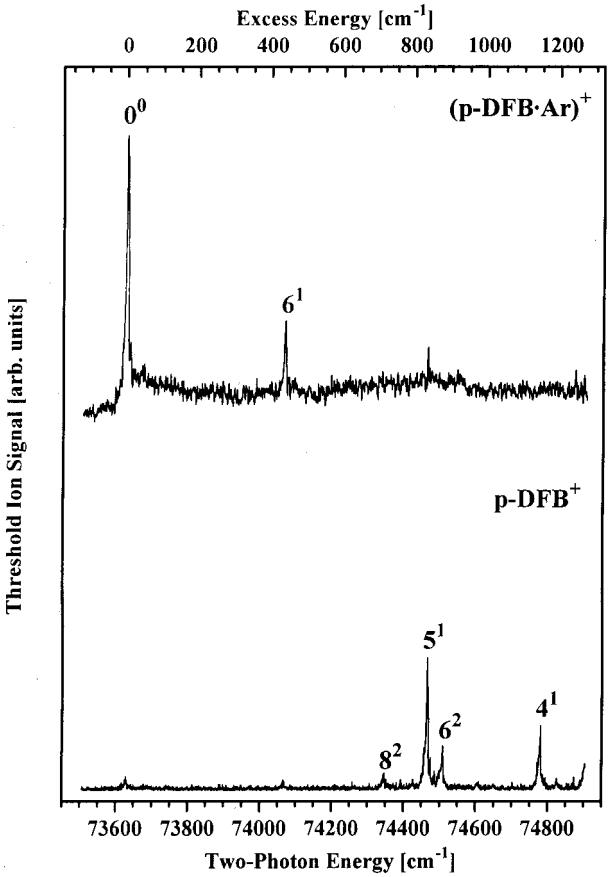

Figure 4. Threshold ion spectra of $(p\text{-DFB}\cdot\text{Ar}_1)^+$, recorded in the mass channels of the ionized complex (upper trace) and of the fragment $p\text{-DFB}^+$ (lower trace) after excitation of the vibrationless intermediate state $S_1 0^0$ of the complex.

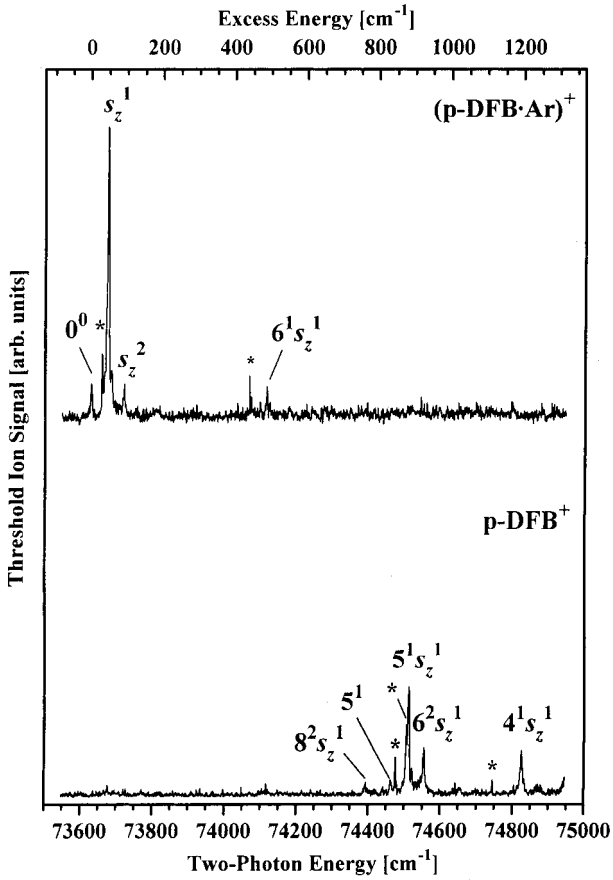

Figure 5. Threshold ion spectra of $(p\text{-DFB}\cdot\text{Ar}_1)^+$, recorded in the mass channels of the ionized complex (upper trace) and of the fragment $p\text{-DFB}^+$ after excitation of the intermolecular stretching vibration s_z^1 in the S_1 state. S_1 resonances, which exhibit very sharp bands, are marked by asterisks.

Ar. The spectra recorded via the $S_1 5^1$ and $S_1 6^2$ intermediate states, however, were recorded with a gas mixture of about 17% Ar in He.

Figure 4 shows the threshold ion spectra of the cationic $p\text{-DFB}\cdot\text{Ar}_1$ complex (upper trace) as well as of its fragment $p\text{-DFB}^+$ (lower trace). Both spectra have been recorded simultaneously after excitation of the vibrationless $S_1 0^0$ intermediate state of the complex. The width of the bands amounts to about 9 cm^{-1} (fwhm). The band of the vibrationless cationic ground state appears at a field-corrected two-photon energy of 73 634 ± 5 cm^{-1}. Compared to the *p*-DFB monomer, this corresponds to a red shift of the adiabatic ionization energy of about 237 cm^{-1}. A very weak band appears about 9 cm^{-1} to the blue side of the 0^0 band, which may be ascribed to the intermolecular bending mode b_y in the ionized complex. Both intramolecular bending modes are symmetry-forbidden. But analogous to the S_1 state, the bending mode b_y perpendicular to the symmetry axis of the chromophore (F−F axis) gains its intensity by a *Herzberg−Teller* coupling of electronic and vibrational degrees of freedom. The 6^1 band is observed at an internal energy of 440 cm^{-1}. Another band in the spectrum of the ionized complex appears at about 836 cm^{-1}. In further measurements, the intensity of this band turned out to be extremely dependent on the experimental conditions such as the irradiance of the ionizing laser or the He/Ar mixing ratio of the carrier gas. In addition, a splitting of the band could be resolved. These observations point to a not fully suppressed S_1 resonance. A comparison of the photon energy of the ionizing laser with the band positions in the R2PI spectra of *p*-DFB and $p\text{-DFB}\cdot\text{Ar}_1$ shows that only the $S_1 \leftarrow S_0$ transitions 5_0^1 and 6_0^2 of the monomer coincide in energy with this band. The appearance of a S_1 resonance of the monomer in the mass channel of the complex is unusual. It could only be explained by the capture of a thermalized photoelectron into a Rydberg state of $p\text{-DFB}\cdot\text{Ar}_1^+$. From this discussion it follows that the 6^1 level has the highest vibrational energy observed in the mass channel of the cationic $p\text{-DFB}\cdot\text{Ar}_1$ complex. All missing bands at higher energy, expected from the spectrum of the isolated *p*-DFB, appear in the MATI spectrum of the fragment $p\text{-DFB}^+$. The fragment bands could be assigned to the vibrational levels 8^2 (717 cm^{-1}), 5^1 (836 cm^{-1}), 6^2 (879 cm^{-1}) and 4^1 (1150 cm^{-1}). Analogous to the 0_0^0 transition, a small peak is observed 9 cm^{-1} above the 5^1 band, which is assigned to the combination band $5^1 b_y^1$. Since the energy of mode ν_5 of the ionized complex coincides with that of the monomer resonances $S_1 5^1$ and $S_1 6^2$, the 5^1 band must be superposed by these resonances. This would also explain its relatively high intensity. The weak ion signal observed in the fragment spectrum in the region of the transitions 0_0^0 and 6_0^1 is due to the fragmentation of the cationic complex as a result of an undesired three-photon absorption (see ref 9).

The threshold ion spectra of $p\text{-DFB}\cdot\text{Ar}_1$ recorded after the excitation of the intermolecular stretching vibration is shown in Figure 5. As expected from the propensity rule, the most intense band in the spectrum recorded in the mass channel of $(p\text{-DFB}\cdot\text{Ar}_1)^+$, appearing 46.5 cm^{-1} above the adiabatic ionization energy, is due to the excitation of the stretching vibration s_z^1 in the cation. In addition, also the first overtone of this mode is observed at about 92 cm^{-1}. The stretching vibration is also

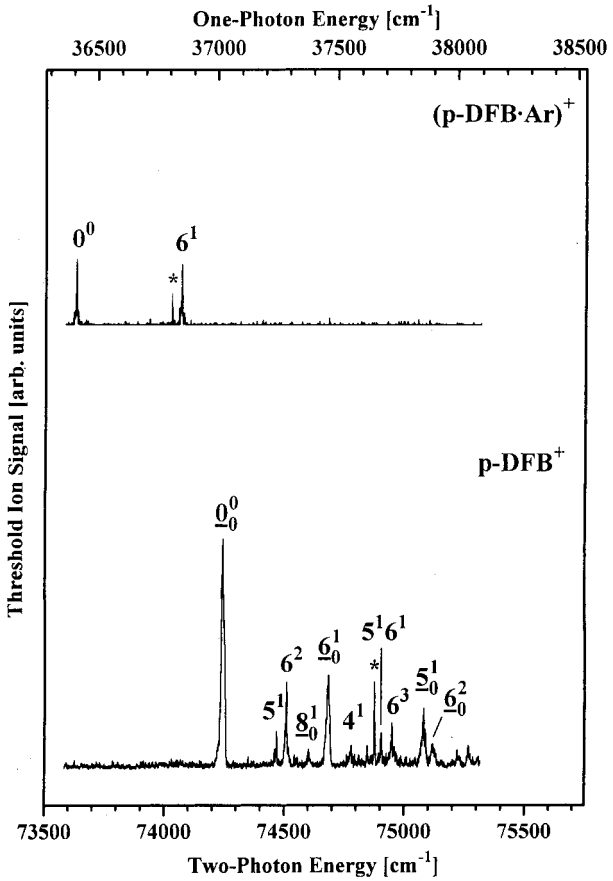

Figure 6. Threshold ion spectra of (*p*-DFB·Ar$_1$)$^+$, recorded in the mass channels of the ionized complex (upper trace) and of the fragment *p*-DFB$^+$ after excitation of the vibrational mode ν_6 in the S_1 state of the complex. S_1 resonances are marked by asterisks. The broad bands (∼17 cm^{-1}, fwhm) in the spectrum of the fragment *p*-DFB$^+$ are due to the vibrationally induced predissociation (VP) of the complex in the S_1 state.

observed in combination with the intermolecular bending mode b_y, however, it can only be resolved for the fundamental stretching vibration. A very sharp resonance is observed just below the s_z^1 vibration. It is assigned to the $S_1 \leftarrow S_0$ 0_0^0 transition of the complex. In this case, the "ionizing" laser induces the $S_1 \leftarrow S_0$ excitation transition, while the ionization is actually caused by the "excitation" laser. Analogously, the band at an excess energy of about 440 cm^{-1} can be ascribed to the $S_1 \leftarrow S_0$ 6_0^1 transition. Unfortunately, the cationic mode ν_6 lies within the same region and thus is covered by this band. The band at 487 cm^{-1}, however, is clearly due to the $6^1 s_z^1$ level. At higher excess energies, no more transitions are observed in the mass channel of the van der Waals complex. The missing bands appear in the MATI spectrum of the fragmentation channel, i.e., that of the fragmentation product *p*-DFB$^+$ (lower trace). The spectrum of the latter still reflects the cluster precursor since the intramolecular vibrational modes appear in combination with the intermolecular stretching vibration s_z. The cationic state with the lowest vibrational energy in the spectrum of the fragment *p*-DFB$^+$ appears at 764 cm^{-1} and is assigned to the combination band $8^2 s_z^1$. Again, the sharp peaks marked by asterisks are due to S_1 resonances.

Exciting the ν_6 in the S_1 state gives rise to the spectra shown in Figure 6. Except for the excitation of the vibrationless cationic ground state and the 6^1 level, no further transitions are observed in the mass channel of the complex. The band at 399 cm^{-1} is due to the S_1 resonance 0_0^0 of *p*-DFB·Ar$_1$.

The spectrum of the fragment *p*-DFB$^+$ (lower trace) shows three different band types, characterized by different bandwidths. The sharpest bands exhibit a width of about 2.5 cm^{-1} (fwhm) and are due to S_1 resonances. Bands with a width of 7.5 cm^{-1} correspond to fragmentation processes in the cationic state of the *p*-DFB·Ar$_1$ complex, which dissociate owing to the high excess energy in the ion. Most striking, however, are bands with a width of about 17.5 cm^{-1}, which are also much more intense compared to the remaining bands. By comparing the fragment spectrum with the *p*-DFB monomer spectra, we could find some corresponding transitions. Thus the broad bands observed in the fragment spectrum of *p*-DFB·Ar, excited via the $S_1 6^1$ intermediate state, correspond to the MATI spectrum of the monomer ionized via the $S_1 0^0$ state (see Figure 2). Analogous to the broad band observed in the fragment spectrum of FB·Ar$_1$,[22] these bands could be clearly ascribed to the vibrational predissociation of the complex in the vibrationally excited intermediate state $S_1 6^1$. After the fragmentation, the chromophore is in the $S_1 0^0$ state from which it is subsequently ionized. Similarly, based on the threshold ion spectrum of the *p*-DFB monomer recorded via the vibrationless $S_1 0^0$ intermediate state, we may assign these "predissociation bands" (VP bands) of the *p*-DFB·Ar complex to the transitions $\underline{0}_0^0$, $\underline{8}_0^1$, $\underline{6}_0^1$, $\underline{5}_0^1$, and $\underline{6}_0^2$, starting in the vibrationless $S_1 \underline{0}^0$ state of the fragment. For a clear distinction between bands arising due to the fragmentation of the ionized complex and those due to the predissociation of the vibronically excited complex, the numerals of the monomer vibrational modes are underlined.

It should be pointed out that here the relative band intensities correspond to those found in the ZEKE-PES measurements. Obviously, 600 cm^{-1} above the ionization limit, ZEKE and MATI spectra are almost identical, owing to the lifetime stabilizing effect of the direct ions on the Rydberg states.

Figure 7 shows the threshold ion spectra of *p*-DFB·Ar$_1$ obtained after ionization via the $S_1 5^1$ intermediate state. In the spectrum of the complex, one essentially observes the band of the vibrationless cationic ground state as well as the 6^1 band. In addition, the intermolecular bending mode b_y is not well-resolved, with a distance of about 9 cm^{-1} above both of these transitions. The extremely weak band at an internal energy of about 303 cm^{-1} is assigned to the vibrational mode ν_{17}. As before, the sharp band above the 6^1 band, marked by an asterisk, is very sensitive to the experimental conditions (vide supra) and thus can be ascribed to the $S_1 \leftarrow S_0$ 0_0^0 transition in the complex with subsequent resonant ionization.

On the basis of the monomer spectrum recorded via the $S_1 5^1$ intermediate state, most of the bands appearing in the spectrum of the *p*-DFB$^+$ fragment channel (lower trace in Figure 7) could be easily assigned to the corresponding vibrations of the ionized chromophore in the complex. The band with the lowest excess energy above the cationic fragmentation threshold is assigned to the $6^1 17^1$ state (744 cm^{-1}). The weak ion signal at the adiabatic ionization energy is due to multiphoton processes. The extraordinary strong fragment signal in the region of the 6^1 band could be rationalized, in addition to multiphoton processes, by the field-induced fragmentation of the complex as has been discussed recently for fluorobenzene·Ar$_1$.[38]

As in the case of the excitation of the vibration ν_6 in the intermediate state, exciting the ν_5 also gives rise to very broad bands in the threshold ion spectrum of the fragment *p*-DFB$^+$, caused by the predissociation of the neutral complex. However, these VP bands exhibit extraordinary differences in their bandwidths. These differences indicate a contribution of

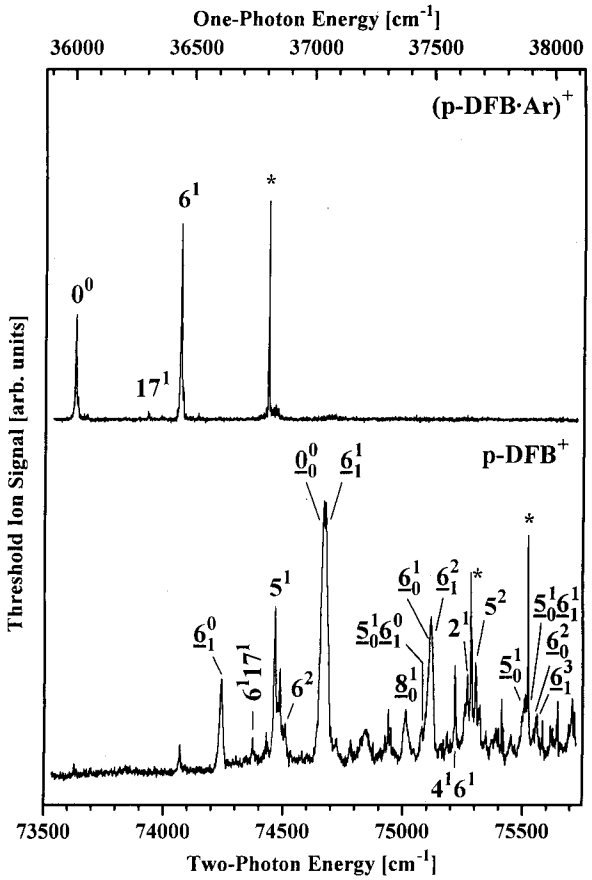

Figure 7. Threshold ion spectra of $(p\text{-DFB}\cdot\text{Ar}_1)^+$, recorded in the mass channels of the ionized complex (upper trace) and of the fragment $p\text{-DFB}^+$ after excitation of the $S_1 5^1$ intermediate state of the complex. S_1 resonances are marked by asterisks. The width of the broad bands in the spectrum of the fragment $p\text{-DFB}^+$ differs extremely from the width of the VP bands in the spectrum recorded via the $S_1 6^1$ state.

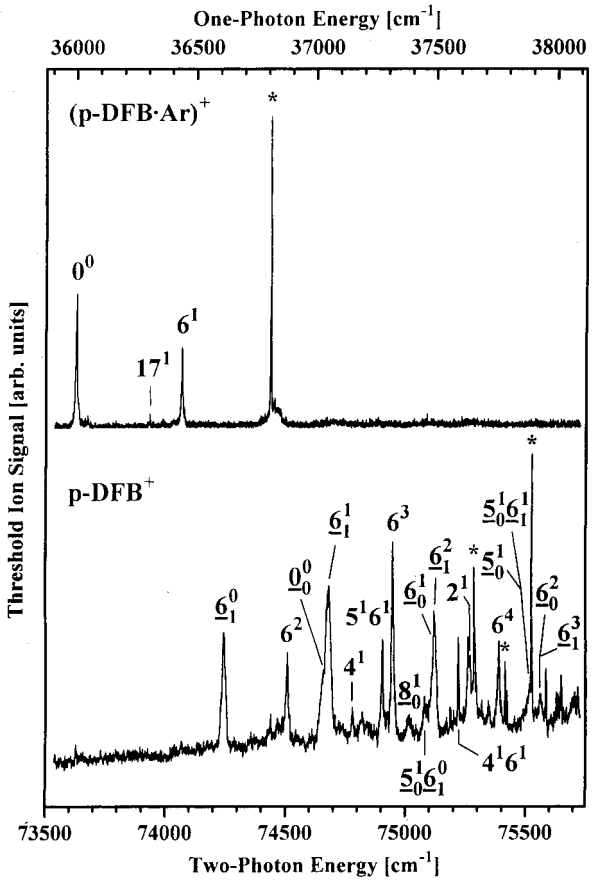

Figure 8. Threshold ion spectra of $(p\text{-DFB}\cdot\text{Ar}_1)^+$, recorded in the mass channels of the ionized complex (upper trace) and of the fragment $p\text{-DFB}^+$ after excitation of the $S_1 6^2$ intermediate state of the complex. S_1 resonances are marked by asterisks. The VP bands exhibit very different band contours compared to those recorded via the $S_1 5^1$ state.

additional fragmentation channels in the vibrationally excited S_1 intermediate state. The lowest VP band at a one-photon energy of the ionizing laser of 36 615 cm^{-1} is about 17.3 cm^{-1} wide (fwhm), which nearly coincides with the width of the VP bands discussed in the preceding sections. A straight comparison with transitions in the free *p*-DFB monomer proves that this band is due to the ionization of the neutral fragment *p*-DFB starting from the $S_1 6^1$ state. Thus this band is assigned to the single transition $\underline{6}_1^0$.

The most intense VP band however appears at a one-photon energy of 37 045 cm^{-1} and is nearly twice as wide (35 cm^{-1}) as the $\underline{6}_1^0$ VP band. In addition, it shows a rudimentary splitting. Such an extreme broadening can only be explained by a superposition of different transitions. Assuming that the $S_1\underline{6}^1$ level of the fragment *p*-DFB is populated by VP of the complex, a band with a "normal" width of about 17 cm^{-1}, corresponding to the $\underline{6}_1^1$ transition, can be quite easily fitted to the higher energy part of the observed band. Analogously, the energetically lower part could be explained by the transition $\underline{0}_0^0$, starting from the vibrationless $S_1\underline{0}^0$ state, into the cationic ground state of the fragment *p*-DFB. The energetic difference of both transitions amounts to about 30 cm^{-1}, which could explain the broadening of the observed VP band. Nevertheless, despite its extraordinary intensity as well as the sufficient separation of the transitions considered (band distance 30 cm^{-1} versus bandwidth ~17 cm^{-1}), both bands could not be resolved.

Another strongly broadened band is observed at a one-photon energy of about 37 491 cm^{-1}. An analysis of this band shows that it is, at least partly, due to the superposition of the transitions $\underline{6}_0^1$ and $\underline{6}_1^2$, also separated by about 30 cm^{-1}. Analogously, the bands at 37 884 and 37 932 cm^{-1} can be ascribed to the transitions $\underline{5}_0^1/\underline{5}_0^1\,\underline{6}_1^1$ and $\underline{6}_0^2/\underline{6}_1^3$, respectively. Remarkable is the strong band in the region of the $\underline{8}_0^1$ transition at a one-photon energy of 37 385 cm^{-1}. This band must also be due to the superposition of different transitions, since the corresponding band in the spectrum of the free *p*-DFB exhibits much less intensity than the other bands. The band at about 37 452 cm^{-1} is due to the transition $\underline{5}_0^1\,\underline{6}_1^0$.

The threshold ion spectra of the $p\text{-DFB}\cdot\text{Ar}_1$ complex, recorded after excitation of the $S_1 6^2$ intermediate state, which lies just 3.5 cm^{-1} higher than the $S_1 5^1$ state, are shown in Figure 8. Except for the different peak intensities, the $(p\text{-DFB}\cdot\text{Ar}_1)^+$ spectrum corresponds to that shown in Figure 7. The spectrum of the fragment $p\text{-DFB}^+$ (lower trace), however, exhibits significant differences. Analogous to the corresponding monomer spectrum (see Figure 3), a long progression of the vibrational mode ν_6 is observed. Again, the FC maximum is shifted to the third harmonic of the ν_6. Also the combination bands $5^1 6^1$ (1276 cm^{-1}) and $4^1 6^1$ (1590 cm^{-1}) could be identified clearly. The weak band at an internal energy of 1150 cm^{-1} is assigned to the 4^1 level. The 2^1 band at 1640 cm^{-1} is partly covered by a strong S_1 resonance.

The broad bands in the fragment spectrum are analogous to the ionization via the intermediate states $S_1 6^1$ and $S_1 5^1$, due to the vibrationally induced predissociation of the complex in the S_1 state. Likewise, a similar broadening of the bands, due to the superposition of different transitions, is observed. Compar-

ing the VP bands in both spectra (Figure 7 and Figure 8), deviations of the band intensities as well as the band contours are significant. This is most striking for the $\underline{0}_0^0/\underline{6}_1^1$ VP band. The only explanation for this asymmetry is that by exciting different vibrations in the S_1 state of the complex, different predissociation channels are favored, resulting in differently populated S_1 vibrational states of the monomer. This is particularly apparent for the band in the region of the $\underline{8}_0^1$ transition, which is now much weaker than before.

4. Discussion

4.1. The *p*-DFB Monomer. Except for the grater bandwidth (10 cm^{-1}) and the relative intensity of the 0_0^0 transition (see discussion above), the threshold ion spectra of the *p*-DFB monomer recorded via the $S_1 0^0$ and $S_1 6^1$ states are virtually identical to the corresponding ZEKE spectra (<6 cm^{-1}) presented by Reiser et al.[30] The broadening of the MATI bands compared to the ZEKE bands is mainly due to the much stronger electric field for the extraction of the threshold ions, which ionizes all long-lived Rydberg states, while in ZEKE experiments only the highest Rydberg states are ionized. Another factor strongly effecting the bandwidth is, as Reiser et al. demonstrated in their studies, the excitation position in the rotational band contour of the S_1 intermediate state.[30] In contrast to the ZEKE spectra, which were recorded with the laser wavelength tuned to the middle of each S_1 band corresponding to states with low rotational excitation, the threshold ion spectra were recorded by exciting the maximum of the *R*-branches.

The field corrected AIE of 73 871 ± 5 cm^{-1} perfectly agrees with the value determined by the ZEKE studies (73 872 ± 3 cm^{-1}).[30] Analogous to the ZEKE spectra, the threshold ion spectra exhibit an extraordinary strong activity of the vibrational mode ν_6. Even after excitation of the ν_5 in the S_1 intermediate state, the 6^1 band in the threshold ion spectrum is more intense than the 5^1 band. Also apparent is the violation of the propensity rule $\Delta v = 0$. If the ionization is performed via the $S_1 6^1$ intermediate state, the FC maximum is observed for the 6_1^2 transition. An ionization via the $S_1 6^2$ state results in a shift of the FC maximum to the 6^3 band.

4.2. The *p*-DFB·Ar$_1$ Complex. *4.2.1. Evaluation of the Fragmentation Thresholds.* On the basis of ab initio calculations at the MP 2 level, Hobza et al. determined a stabilization enthalpy for the *p*-DFB·Ar_1 complex in the S_0 state of 294 cm^{-1} and a van der Waals bond length of 3.6 Å.[39] R. Sussmann and H. J. Neusser investigated the vibronic bands of the vdW modes above the electronic transition $S_1(B_2) \leftarrow S_0(A_1)$ 0_0^0 of *p*-DFB·Ar_1 up to a vdW excitation energy of 125 cm^{-1} by means of rotationally and mass-resolved R2PI spectroscopy.[34] On the basis of the obtained data, they derived structures for the *p*-DFB·Ar_1 complex in the electronic ground state S_0 and in the electronically excited S_1 state. According to these results, in the S_1 state, the Ar atom should lie 3.55(2) Å above the plane of the ring, on the C_2 axis of *p*-DFB.[40] After the electronic excitation into the S_1 state, the bond length is reduced by 0.06 Å. On the basis of an extrapolation of the anharmonicity of the vdW stretching vibrations s_z^1, s_z^2, and s_z^3, Sussmann and Neusser determined a potential depth of about 300 cm^{-1} in the S_1.[34]

The AIE of the *p*-DFB·Ar_1 complex, determined by the threshold ion measurements shown here, amounts to 73 634 cm^{-1} (vide supra). Thus compared to the *p*-DFB monomer, the AIE is lowered by about 237 cm^{-1}, corresponding to an enhanced stabilization of the complex in the cationic state. The frequencies of the intramolecular vibrational modes of the complex are almost identical to those of the monomer. An upper limit for the fragmentation threshold of the vibrationally excited $(p\text{-DFB·Ar}_1)^+$ can be derived from the first appearance of bands in the spectrum of the fragment channel, corresponding to cationic states of the complex. The vibrational state with the lowest excitation energy above the fragmentation threshold of the cationic complex was observed after the excitation of the vibrationless $S_1 0^0$ intermediate state and has been assigned to the 8^2 band (717 cm^{-1}). Owing to the lowering of the AIE by 237 cm^{-1}, an upper limit for the fragmentation threshold in the electronic ground state D_g is given by 480 cm^{-1} ($D_g = D_+ - \Delta$AIE, see ref 13). Analogously, owing to the shift of the ionization transition IP $\leftarrow S_1 0^0$ (IP: ionization potential) by $\Delta h\nu_{2,IP} = 207$ cm^{-1} (difference of the photon energies), an upper limit for the fragmentation threshold D_e in the electronically excited S_1 state can be calculated, which amounts to 510 cm^{-1} ($D_e = D_+ - \Delta h\nu_{2,IP}$, see ref 13). It should be pointed out that the upper limits for the fragmentation thresholds obtained for the *p*-DFB·Ar_1 complex are much higher than those of the fluorobenzene·Ar_1 complex, which could be determined very precisely.[13,22,38] As shown by the ab initio calculations of Hobza et al.,[39] one would expect similar fragmentation thresholds for *p*-DFB·Ar_1 and FB·Ar_1. The main reason for the relatively high value of the upper limit of D_+ obtained for *p*-DFB·Ar_1 is due to the low density of vibrational states in the energy region where fragmentation sets in. Because of the higher symmetry of *p*-DFB·Ar_1, the change of the equilibrium configuration during ionization is less pronounced than for FB·Ar_1, which means that a development of long vdW progressions is unlikely. In addition, the intermolecular bending modes are of b_1 and b_2 symmetry, respectively. Thus an excitation of these vdW modes in the cationic state is symmetry-forbidden, at least for the intermediate states excited in the MATI measurements presented. The observation of one quantum of the bending mode b_y is due to a strong coupling of electronic and vibrational degrees of freedom (*Herzberg−Teller coupling*), as has already been discussed.

Since vibrational predissociation of the complex in the S_1 state already sets in after the excitation of the ν_6 vibration (410 cm^{-1}), the upper limits for fragmentation can be further reduced. Taking into account the red shift of the $S_1 \leftarrow S_0$ 0_0^0 transition (30 cm^{-1}) and ΔAIE = 237 cm^{-1}, D_g is reduced to 380 cm^{-1} and D_+ to 617 cm^{-1}, respectively.

Lower limits for the fragmentation thresholds can be roughly estimated by inspecting the highest vibrational states of the complex where it is still stable. The energetically highest bands in the MATI spectra of the complex recorded via the intermediate states $S_1 0^0$, $S_1 6^1$, and $S_1 6^2$ correspond to the vibrational mode ν_6 (440 cm^{-1}). After the excitation of the ν_5 in the S_1 state, the cationic mode ν_6 also appears in combination with the intermolecular bending vibration b_y. In spectra with an improved signal-to-noise ratio, the combination band $6^1 b_y^1$ could also be resolved after the ionization via the $S_1 0^0$ state. Hence, lower limits for D_g, D_e, and D_+ are given by 212, 242, and 449 cm^{-1}, respectively.

After the excitation of the intermolecular stretching vibration in the intermediate state, even the combination band $6^1 s_z^1$ at 487 cm^{-1} is observed in the $(p\text{-DFB·Ar}_1)^+$ spectrum. The lower limits are thus further shifted by about 38 cm^{-1}. In summary,

upper and lower limits for the dissociation energies are

$$487\ \text{cm}^{-1} < D_+ < 617\ \text{cm}^{-1}$$

$$280\ \text{cm}^{-1} < D_e < 410\ \text{cm}^{-1}$$

$$250\ \text{cm}^{-1} < D_g < 380\ \text{cm}^{-1}$$

In their first study concerning the mode selectivity of the vibrational predissociation of vdW complexes, Parmenter et al. observed the fragmentation of *p*-DFB·Ar_1 in the vibronically excited $S_1 6^1$ state. From this, they derived an upper limit for the fragmentation threshold D_e in the S_1 state of 410 cm^{-1}. On the basis of an incorrect conclusion, they fixed the lower limit for the fragmentation threshold in the S_0 to 348 cm^{-1}.[1] After a revision of this assignment, they corrected this value to 160 cm^{-1}.[31,32] This latter limit was based on the observation of a s_z progression of type s_{zn}^1 up to the forth quantum in their dispersed fluorescence spectra. In their extended study, they observed a strong fluorescence signal of the free *p*-DFB monomer after the excitation of the $S_1 30^2$ state ($\epsilon_{vib} = 242\ cm^{-1}$) of the complex, which they attributed to the vibrational predissociation of the cluster. From this assignment they determined a new upper limit for the fragmentation threshold D_e in the S_1 state. They also observed the fragmentation of the complex after the excitation of the $S_1 8^2$ state ($\epsilon_{vib} = 376\ cm^{-1}$). Taking into account the red shift of the S_1 band origin of *p*-DFB·Ar_1 with respect to the corresponding transition in the *p*-DFB monomer of 30 cm^{-1}, Parmenter et al. determined the following limits:[31]

$$190\ \text{cm}^{-1} < D_e < 242\ \text{cm}^{-1}$$

$$160\ \text{cm}^{-1} < D_g < 212\ \text{cm}^{-1}$$

These limits deviate considerably from those obtained by the MATI studies presented in this article and also from the energies found for similar clusters in other studies.[9,12,13,22] In summary, the lower limits obtained by the MATI studies lie well above the upper limits given by Parmenter et al. A significantly lower fragmentation threshold of the cation could be deduced from the relatively strong band in the region of the 6^1 level in the fragment spectrum recorded via the $S_1 5^1$ state. But this lowering of the threshold could also be explained analogously to the observations made for the cationic fragmentation of the fluorobenzene·Ar_1 complex by Grebner and Neusser. In their threshold ion spectra, they observed an overlap of bands in the spectra of the complex precursor and the fragment. On the basis of the field-dependence measurements they could rationalize this observation by a field-induced lowering of the fragmentation threshold, due to a *Rydberg*−*Rydberg* coupling.[38]

The development of theoretical models describing simple vdW complexes has greatly advanced in recent years, and binding energies obtained by the best ab initio calculations agree very well with experimentally determined values. For example, the calculated stabilization enthalpy of 295 cm^{-1} for the FB·Ar_1 complex in the S_0 state differs from the experimentally determined value ($D_g \sim 344\ cm^{-1}$, refs 13, 38) only by about 15%.[39] For the *p*-DFB·Ar_1 complex, Hobza et al. determined a similar stabilization enthalpy of 294 cm^{-1}.[39] This value lies within our estimated limits (250 $cm^{-1} < D_g < 380\ cm^{-1}$). Since the s_z vibrations in the S_1 in both cluster systems are very similar (FB·Ar_1, 43 cm^{-1}, see ref 22; *p*-DFB·Ar_1, 42 cm^{-1}), similar binding energies should follow for both clusters. Since no significant change in the binding potential is expected going from FB·Ar_1 to *p*-DFB·Ar_1, the limits determined by the MATI measurements are most reasonable.

4.2.2. Vibrational Predissociation of the Vibronically Excited Complex. Parmenter et al. studied the dynamics of the vibrationally induced predissociation of *p*-DFB·Ar_1 by exciting seven different vibrational levels in the S_1 state of the complex in the range from 200 to 900 cm^{-1} above the 0^0 state.[1,31,32] From their fluorescence spectra they deduced that after the predissociation, six out of the seven vibrational states of the complex studied end up at best in two final states of the fragment *p*-DFB(S_1). These two states should be the vibrationless $S_1 0^0$ and, if energetically accessible, the vibrationally excited $S_1 \underline{6}^1$. Only for the $S_1 29^2$ complex state they observed an additional fragmentation channel into the $S_1 \underline{29}^1$ monomer state. For each excited state of the complex they determined the contribution of the main fluorescence channels (resonant fluorescence of the complex and the fragment) to the integrated fluorescence. Assuming equal fluorescence quantum yields and equal fluorescence rate constants ($k_f = 10^8\ s^{-1}$, ref 33) for *p*-DFB and *p*-DFB·Ar for all levels studied, they determined state-to-state VP rate constants k_{VP} for each fragmentation channel. A detailed analysis showed that the VP lifetimes and therefore the VP process are extremely dependent on the excited mode in the S_1 state of the complex. The most remarkable aspect emerging from these studies is that the vibrationally induced predissociation of the $S_1 5^1$ state takes place much faster than that of the $S_1 6^2$ state, although the excess energies differ only by about 3 cm^{-1}.[31]

Jacobson, Humphrey, and Rice determined the VP lifetimes of 12 different S_1 states of the *p*-DFB·Ar_1 complex in a more direct way by means of time-resolved two-photon ionization spectroscopy.[2] They could demonstrate that even at very high excess energies (far more than 1000 cm^{-1}) the vibrational predissociation behaves nonstatistically. The rate constants exhibit no clear relationship to the excitation energy, which would be expected for a statistical fragmentation process. Even in the case of a direct excitation of the intermolecular stretching vibration, i.e., the reaction coordinate, the rate constants behaved counterintuitive and scattered extremely. For example, the vibrationally excited complex in the $S_1 5^1 s_z^1$ state dissociates only about half as fast as in the $S_1 5^1$ state. On the other hand, for a complex in the $S_1 6^2 s_z^1$ state a much shorter lifetime than in the $S_1 6^2$ state was observed.[2]

As has been described in the previous sections, some VP bands in the threshold ion spectra of *p*-DFB·Ar_1 seem to be much too intense and do not exhibit a band contour as would be expected from the superposition of only two fragmentation channels. For a more detailed analysis of the VP bands observed in the threshold ion spectra of the fragment, the spectra were normalized to the energy of the ionizing laser and slightly smoothed. Furthermore, the rising baseline in the spectra was subtracted. The resulting spectra are shown in Figures 9−11. An additional aspect should be pointed out. It is remarkable that both the VP bands as well as the bands of the complex, fragmented in the ionic state, are observed in the same fragment MATI spectra. This is due to the fact that the fragmentation of the vibronically excited complex is determined by two separate processes. First an intramolecular/intracluster vibrational energy redistribution (IVR) from the excited states of the chromophore to the van der Waals modes of the complex takes place, before the actual VP process occurs. As has been established for several complexes, the rate-determining step is the IVR process.[15−17,41,42] The presented spectra have been recorded with

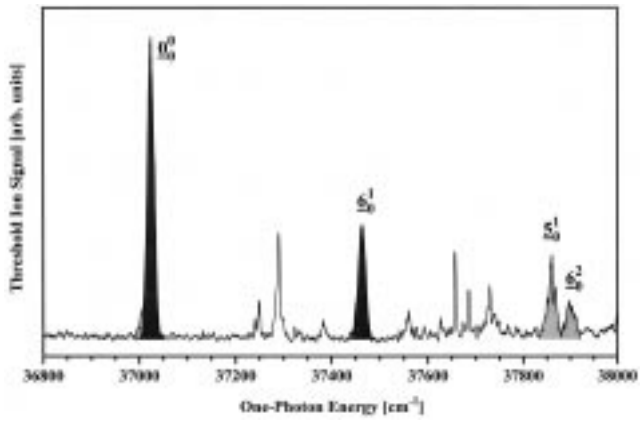

Figure 9. Clipping of the fragment spectrum of *p*-DFB·Ar_1, which was recorded after the excitation of the intermediate state $S_1 6^1$. In this representation, the spectrum has been normalized to the intensity of the ionizing laser and slightly smoothed. The broad VP bands are emphasized by a light shading. The bands $\underline{0}_0^0$ as well as $\underline{6}_0^1$ have been fitted by Gaussian curves (dark shading).

a temporal overlap of the two laser pulses of about 3 ns. Since both band types could be observed at the same time, the lifetime of the excited complex must lie in the same order.

The lowest vibrational state in the S_1, for which VP bands have been observed in the threshold ion spectra of the fragment p-DFP^+, corresponds to the 6^1 band (410 cm^{-1}). Figure 9 shows a clipping of the corresponding fragment spectrum. One striking characteristic of the VP bands is their bandwidth of about 17 cm^{-1}, which makes it rather easy to distinguish them from vibrational bands stemming from the fragmentation of the cationic cluster. Compared to the large bandwidth of a VP band, observed earlier for FB·Ar_1 in the S_1 state ($\sim$28 cm^{-1}), the width of the *p*-DFB·Ar_1 VP bands are considerably narrower. The enormous width of the VP bands must be due to the rotational excitation of the fragment by the predissociation process.[15,17] The reduced bandwidth compared to the VP band observed for FB·Ar_1 can be rationalized by the higher symmetry of the *p*-DFB·Ar_1 complex. Owing to the transition energies (photon energy of the ionizing laser), all VP bands, without exception, could be assigned to transitions of the *p*-DFB monomer starting from the vibrationless $S_1 \underline{0}^0$ state. The contour of the bands corresponding to the transitions $\underline{0}_0^0$ and $\underline{6}_0^1$ may be fitted very well by *Gaussian* curves. The relative intensity of these bands correspond to those determined in ZEKE spectra.[30]

Considerably more difficult was the analysis of the spectra recorded via the $S_1 5^1$ intermediate state (see Figure 10). The first VP band appears at a much lower transition energy than before. A comparison with the threshold ion spectra of the monomer reveals that this band is due to the $\underline{6}_1^0$ transition into the vibrationless cationic ground state, starting from the vibrationally excited S_1 state of the *p*-DFB fragment. As before, this band can also be fitted by a *Gaussian* contour and its width is almost the same as that of the VP bands in the spectrum in Figure 9. Thus it has to be due to a single transition. The bands at 37 045 and 37 491 cm^{-1}, however, are much broader (35 and 28 cm^{-1}) and exhibit an asymmetric contour. Both bands may only be rationalized by the superposition of different transitions. To corroborate this conclusion, first of all it must be checked whether bands of the ionized complex could distort these VP bands. Inspecting the monomer spectra reveals that no cluster transitions with significant intensity should lie in the corresponding energy region. As has been discussed before, the flank on blue side of the broad VP bands is obviously due to the excitation of a progression of the vibrational mode ν_6 in the cationic fragment. For this reason, the blue-sided flanks of these bands were fitted at first with Gaussian contours of maximum intensity, corresponding to the transitions $\underline{6}_1^1$ and $\underline{6}_1^2$, respectively. In this way, the flanks could be simulated very well. However, the relative intensities do not coincide with that of the corresponding transitions observed in the threshold ion spectra of the monomer. For example, after the ionization via the $S_1 \underline{6}^1$ state of the monomer, the maximum of the FC factors should be shifted to the $\underline{6}_1^2$ transition. For this reason, the contribution of the $\underline{6}_1^1$ band has been reduced

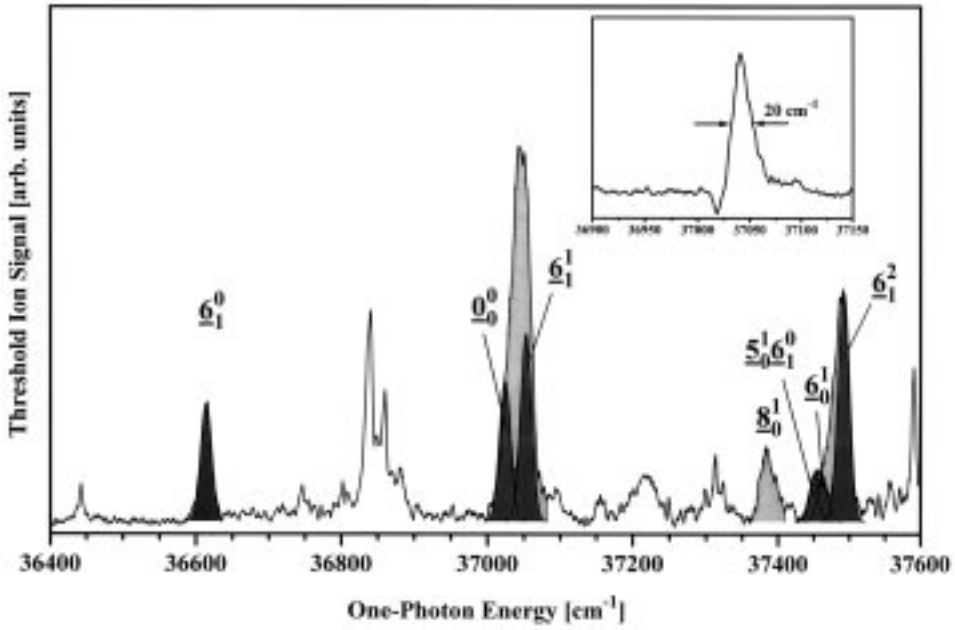

Figure 10. Clipping of the fragment spectrum of *p*-DFB·Ar_1, recorded via the intermediate state $S_1 5^1$. The spectrum has been normalized to the intensity of the ionizing laser and slightly smoothed. In addition, the shallow increase of the baseline has been subtracted. Again, the broad VP bands are emphasized by a light shading. The inset shows an artificial spectrum in the region of about 37 050 cm^{-1}, for which the Gaussian fits for the VP bands $\underline{0}_0^0$ and $\underline{6}_1^1$ have been subtracted from the recorded spectrum.

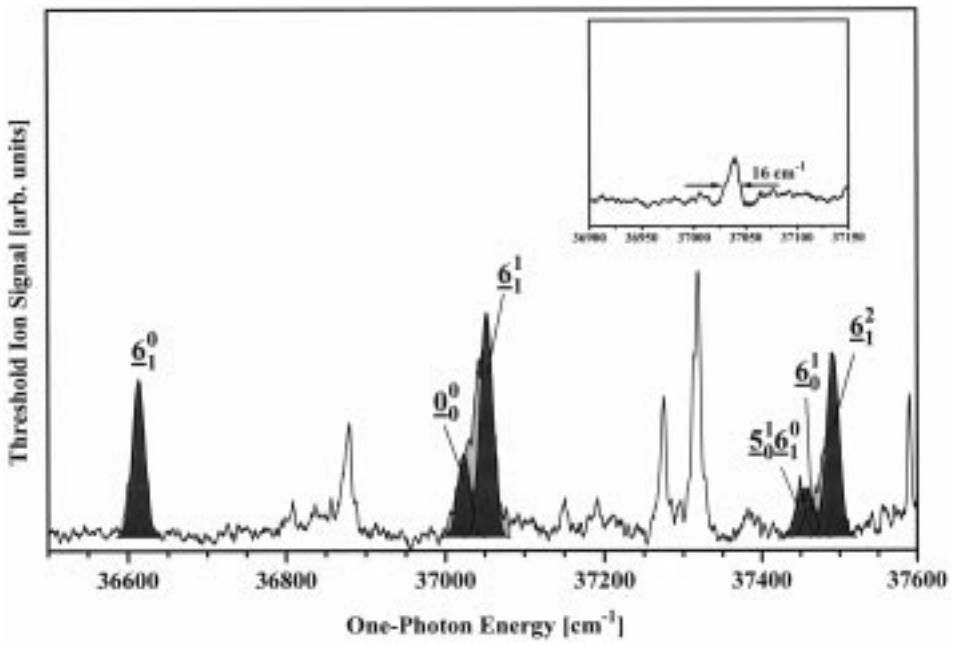

Figure 11. Clipping of the fragment spectrum of *p*-DFB·Ar$_1$, recorded via the intermediate state $S_1 6^2$. The spectrum has been normalized to the intensity of the ionizing laser and slightly smoothed. In addition, the slow increase of the baseline has been subtracted. The VP bands are fitted by Gaussian curves (dark shading) with maximum intensity. The inset shows the calculated difference spectrum in the region of the $\underline{0}_0^0/\underline{6}_1^1$ VP band. The resulting band exhibits about the typical VP bandwidth.

analogously to the relative intensities observed in the corresponding monomer spectrum (see Figure 2).

The energetically lower part of the VP band at 37 045 cm^{-1} is, at least partly, due to the transition $\underline{0}_0^0$, starting in the vibrationless S_1 state of the monomer. Obviously, besides a dissociation resulting in a *p*-DFB fragment in the $S_1\underline{6}^1$ state, also a decay into the $S_1\underline{0}^0$ state exists. Consequently, the transition $\underline{6}_0^1$ must lie underneath the broad band at 37 491 cm^{-1}. One may also deduce from the MATI spectrum of the monomer excited via the $S_1 6^1$ intermediate state, that the transition $\underline{5}_0^1\,\underline{6}_1^0$ should fall into this energy region, resulting in an additional broadening of the band in the lower part.

It is apparent that the broad VP bands (light shading) cannot be rationalized completely by the identified transitions (dark shading). Particularly if the relative intensities of the transitions in the monomer spectrum are taken into account for the Gaussian fits, about 50% of the most intense VP band could not be covered. The inset in Figure 10 shows the difference spectrum in the region around 37 050 cm^{-1}, for which the Gaussian fits for the VP bands $\underline{0}_0^0$ and $\underline{6}_1^1$ have been subtracted from the recorded spectrum. The calculated spectrum exhibits a band of significant intensity and a width of about 20 cm^{-1} (fwhm), somewhat broader than a typical single VP band. Even in the case of a maximum fit, discussed above, the uncovered region still amounts to nearly 30% of the band. Also 20% of the second broadened band could not be rationalized by bands from the exit channels $S_1\underline{0}^0$ and $S_1\underline{6}^1$ of the fragment. The only explanation is that additional fragmentation channels must exist, resulting in different final states of the monomer. Energetically, a large series of S_1 states of the monomer could be populated after VP (see Figure 13), from which then an ionization transition could be induced. From the known monomer transitions, the $\underline{17}_1^1$ ($\Delta E = 29$ cm^{-1}, relative to the $\underline{0}_0^0$ transition), $\underline{27}_1^1$ (27 cm^{-1}), $\underline{30}_1^1$ (7 cm^{-1}), $\underline{30}_2^2$ (14 cm^{-1}) and $\underline{30}_3^3$ (21 cm^{-1}) fall into this region of the overlapping $\underline{0}_0^0/\underline{6}_1^1$ bands. So from the shift of the unknown "difference band" in the insert of Figure 10 the $\underline{30}_n^n$ ($n = 1, ..., 3$) are good candidates.

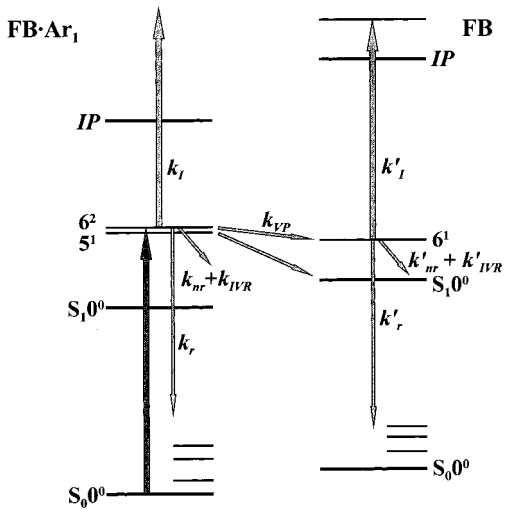

Figure 12. Decay processes of the vibrationally excited S_1 state of the *p*-DFB·Ar$_1$ complex. Apart from the predissociation of the complex with the rate constant k_{VP}, the originally excited states are depopulated by radiative and nonradiative decay processes with rate constants k_r and k_{nr}, respectively. In addition, intramolecular vibrational redistribution of the excess energy can occur with a rate constant k_{IVR}. The intramolecular relaxation processes (rate constants: k'_r, k'_{nr}, k'_{IVR}) are also relevant for the depopulation of the fragment states, populated by the predissociation of the complex. Thus by means of ionization (rate constants k_I and k'_I), only the remaining states of the complex and the fragment will be detected.

Exciting the intermediate state $S_1 6^2$ of the *p*-DFB·Ar$_1$ complex, the observed VP bands are essentially due to transitions starting in the monomer states $S_1\underline{0}^0$ and $S_1\underline{6}^1$, respectively. In contrast to the VP spectra recorded via the $S_1 5^1$ state of the complex, the superposed VP bands are now much more asymmetric and exhibit a distinctively different intensity distribution (see Figure 11). The lowest band at 36 613 cm^{-1} is again due to the $\underline{6}_1^0$ transition. The blue side of the wide VP bands can be approximated very well by Gaussian fits, corresponding to the transitions $\underline{6}_1^1$ and $\underline{6}_1^2$, respectively. In addition,

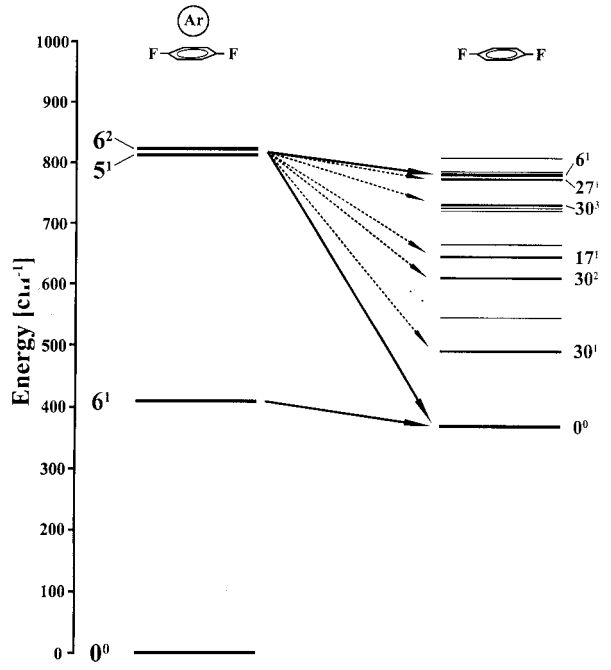

Figure 13. Schematic diagram of the S_1 states of *p*-DFB·Ar_1. The main fragmentation channels into the final monomer states are indicated by heavy arrows. Additional fragmentation channels, which could not be determined quantitatively, are indicated by pointed arrows. The binding energy in the S_1 state was, analogously to the FB·Ar_1 complex, estimated by about 370 cm^{-1}.

the monomer transitions $\underline{0}_0^0$, $\underline{6}_0^1$ as well as $\underline{5}_0^1\,\underline{6}_1^0$ have been fitted with maximum intensity (see Figure 11). In contrast to the former spectrum, after the summation of these transitions, the VP bands are covered much better. The difference for the $\underline{0}_0^0/\underline{6}_1^1$ band only amounts to about 20% and for the $\underline{5}_0^1\,\underline{6}_1^0/\underline{6}_0^1\underline{6}_1^2$ band even less than 4%. Again, the inset in Figure 11 shows the calculated difference spectrum in the region of the $\underline{0}_0^0/\underline{6}_1^1$ VP band. The resulting band is now much smaller than before, and it exhibits the typical VP bandwidth. This clearly indicates that additional fragmentation channels apart from VP into the final states $S_1\underline{0}^0$ and $S_1\underline{6}^1$ of the monomer play a minor role in the predissociation of the S_16^2 state of the complex. The relative intensities of the $\underline{6}_1^0$ and $\underline{6}_1^1$ bands correspond to those, observed in the spectrum of the free *p*-DFB monomer in Figure 2. Only the $\underline{6}_1^2$ band is definitely too weak, which could not be rationalized by the existing data up to now.

For an interpretation of the observed relative VP band intensities, it is important to have a look at the processes that are responsible for the depletion of an initially populated state. There are several different, simultaneous processes, which result in a reduction of the population of an initially excited vibrational state in the S_1 of the *p*-DFB·Ar_1 complex (see Figure 12). Essentially, these are

(i) radiative decay with the rate constant k_r,

(ii) nonradiative decay with the rate constant k_{nr},

(iii) transitions between vibrational states of the complex ("intramolecular vibrational redistribution", IVR) with the rate constant k_{IVR},

(iv) ionization of the complex with the rate constant k_I, and

(v) vibrationally induced predissociation of the complex with the rate constant k_{VP}.

Except for the vibrational predissociation, these relaxation processes are also relevant for the states of the fragment populated after the predissociation of the complex (rate constants: k_r', k_{nr}', k_{IVR}', k_I').

The intensity of the VP bands depends on the concentration of the vibronically excited *p*-DFB monomer, produced after predissociation of the *p*-DFB·Ar_1 complex. Analogous to the depletion of the states of the complex, the initially populated S_1 states of the fragment are depleted by radiative and nonradiative decay before the ionization takes place. But owing to the lower density of states in the monomer, IVR should be reduced drastically compared to IVR in the complex. Particularly crucial to the observed intensities are the Franck−Condon factors of the transitions. In addition, if one intends to compare band intensities of transitions observed in different measurements, the spectral energy distribution $\rho(\bar{\nu})$ of the ionizing laser has to be taken into account. Thus, assuming that the rate constants for the different decay processes are time independent, the intensity of a transition, starting in the VP-populated S_1 state of the monomer with the vibration $\underline{\upsilon}'$ and resulting in the cationic state with the mode $\underline{\upsilon}$ excited, is given by

$$I_{VP}(\underline{\upsilon}' \rightarrow \underline{\upsilon}, t) \sim c_0 \cdot f_{\upsilon \rightarrow \underline{\upsilon}'} \cdot \exp[-(k_r' + k_{nr}') \cdot t] \cdot \rho(\bar{\nu}) \cdot |\langle \psi_{\underline{\upsilon}'} | \psi^+_{\underline{\upsilon}} \rangle|^2$$

Here c_0 denotes the initial total concentration of *p*-DFB in the electronically excited S_1 state, produced by VP of the *p*-DFB·Ar_1 complex. The predissociation from a vibrational state υ of the complex into the final state $\underline{\upsilon}'$ of the fragment, i.e., the relative population of different final vibrational states, is taken into account by the branching ratio $f_{\upsilon \rightarrow \underline{\upsilon}'}$.

In the preceding analysis of the fragment ion spectra it has been shown that the width and the contour of the VP bands is extremely sensitive to which S_1 state the complex is initially excited. We have also given evidence that this is caused by the superposition of different transitions into the cationic states, starting from different VP product states. For a direct comparison of our results with those of Parmenter et al., it would be interesting to determine the branching ratios $f_{\upsilon \rightarrow \underline{\upsilon}'}$ for the predissociation from a mode υ of the complex to a mode $\underline{\upsilon}'$ of the fragment. But since the FC factors of the transitions into the cationic states as well as the initial concentration c_0 of vibronically excited *p*-DFB are unknown, the determination of the absolute branching ratios is impossible. For this reason, we alternatively compared the relative band intensities $I_{VP}(\underline{6}_1^1)/I_{VP}(\underline{0}_0^0)$ for the intermediate states S_15^1 and S_16^2 of the complex, to make a rough estimate for the different populations. The intensity relation of the VP bands $\underline{6}_1^1$ and $\underline{0}_0^0$ after excitation of the S_15^1 state is given by

$$\frac{I_{VP}(\underline{6}_1^1)}{I_{VP}(\underline{0}_0^0)} = \frac{f_{5^1 \rightarrow \underline{6}^1}}{f_{5^1 \rightarrow \underline{0}^0}} \cdot \frac{\exp[-(k_r'(\underline{6}^1) + k_{nr}'(\underline{6}^1)) \cdot t]}{\exp[-(k_r'(\underline{0}^0) + k_{nr}'(\underline{0}^0)) \cdot t]} \cdot \frac{FCF(\underline{6}_1^1)}{FCF(\underline{0}_0^0)}$$

and analogously for the excitation of the S_16^2 state by

$$\frac{I_{VP}(\underline{6}_1^1)}{I_{VP}(\underline{0}_0^0)} = \frac{f_{6^2 \rightarrow \underline{6}^1}}{f_{6^2 \rightarrow \underline{0}^0}} \cdot \frac{\exp[-(k_r'(\underline{6}^1) + k_{nr}'(\underline{6}^1)) \cdot t]}{\exp[-(k_r'(\underline{0}^0) + k_{nr}'(\underline{0}^0)) \cdot t]} \cdot \frac{FCF(\underline{6}_1^1)}{FCF(\underline{0}_0^0)}$$

If we now consider the quotient of the two relative band intensities taken from the spectra recorded via the S_15^1 and the S_16^2 state, also the FC factors as well as the exponential factors, which contain the rate constants k_r' and k_{nr}', will be eliminated and we obtain

$$\frac{I_{S_16^2}(\underline{6}_1^1)}{I_{S_16^2}(\underline{0}_0^0)} \Big/ \frac{I_{S_15^1}(\underline{6}_1^1)}{I_{S_15^1}(\underline{0}_0^0)} = \frac{f_{6^2 \rightarrow \underline{6}^1}}{f_{6^2 \rightarrow \underline{0}^0}} \Big/ \frac{f_{5^2 \rightarrow \underline{6}^1}}{f_{5^1 \rightarrow \underline{0}^0}}$$

For an evaluation of this expression in the present structure, the areas beneath the Gaussian curves corresponding to the transitions $\underline{0}_0^0$ and $\underline{6}_1^1$ have been determined. From the spectrum, recorded via the $S_1 5^1$ complex state, the intensity relation of the bands $\underline{6}_1^1$ and $\underline{0}_0^0$ amounts to about 1.3 for the corrected band intensities. After excitation of the $S_1 6^2$ complex state, the $\underline{6}_1^1$ transition is about 2.7 times more intense than the $\underline{0}_0^0$ transition and thus:

$$\frac{f_{6^2\rightarrow\underline{6}^1}}{f_{6^2\rightarrow\underline{0}^0}} \Big/ \frac{f_{5^1\rightarrow\underline{6}^1}}{f_{5^1\rightarrow\underline{0}^0}} = 2.1$$

Provided that the intensity of the $\underline{6}_1^1$ Gaussian curve has been adapted correctly, this means that there is a much stronger propensity for the population of the $S_1\underline{6}^1$ final state of the fragment by exciting the $S_1 6^2$ state than by exciting the $S_1 5^1$ state of the complex. This strong mode selectivity is surprising insofar as the difference of the vibrational excess energies only amounts to about 3 cm^{-1}.

From the rate constants or branching ratios, determined by Parmenter et al., the above ratio is even larger, giving a value of about 5. In their studies based on UV fluorescence spectroscopy, these authors could show that the lifetimes for the vibrationally induced predissociation process as well as the redistribution of the vibrational energy depends drastically on the initial vibration, excited in the S_1 state of the complex.[1,31,32] In their first paper, they compared their results with the predictions of the *half-collision* model and the *energy/momentum gap* model. Although the half-collision model does not take into account the consecutive character of the IVR/VP process, some predictions of this model are interesting in regard to the results of our MATI measurements. Therefore, it is discussed here briefly.

In the half-collision model, the predissociation of a complex is considered to be the second half of the vibrational energy transfer in a *full-collision*.[1] Encouraged by the success of the full-collision model, describing the mode-to-mode vibrational energy flow in S_1 benzene[43] and *p*-DFB[44] in a bulb experiment at 300 K, Parmenter et al. attempted to reproduce the experimentally observed VP energy flow probabilities of *p*-DFB·Ar by using this model and its propensity rules. The relative probability P_{ab} for a vibrational energy transfer, in which only modes a and b undergo quantum changes, is given by[1,43]

$$P_{ab} = V_a^2\, V_b^2 I(\Delta E)$$

The factors V^2 impose the restrictions due to quantum number changes and depend on the magnitude $|\Delta\nu|$ of the quantum change of each mode (for more detail see ref 43). For collisions of Ar with *p*-DFB, these factors are very similar for all modes except for the out-of-plane mode ν_{30}:[44]

$$V_a{}^2 = V_b{}^2 = \ldots = (0.1)^{|\Delta\nu|} \quad \text{and} \quad V_{30}^2 = (0.6)^{|\Delta\nu|}$$

The factor I in the above formula mainly depends on the energy gap ΔE between the initial and the final state. Only a small variation of the factor $I(\Delta E)$ is found both for different systems and different modes.[43] For the energy ΔE being transferred between vibrational and translational/rotational degrees of freedom in VP, the factor $I(\Delta E)$ is roughly given by[1,43]

$$I(\Delta E) = 0.6 \quad \text{for} \quad \Delta E < 50\ cm^{-1}$$

$$I(\Delta E) = \exp[-10^{-2}(\Delta E)] \quad \text{for} \quad \Delta E > 50\ cm^{-1}$$

From the half-collision model Parmenter's group could derive a strong selectivity with respect to the final states of the fragment, but it was not possible to reproduce the experimentally observed branching ratios. For example, the values predicted by the half-collision model for the predissociation into the $S_1\underline{0}^0$ monomer final state was extraordinarily small (0.2% and 2.9%, respectively) compared to the experimentally observed contribution of about 18% (after $S_1 6^2$ excitation) and 52% (after $S_1 5^1$ excitation), respectively.[1] On the other hand, it should be pointed out that the half-collision model predicts relatively strong propensities for some fragmentation channels, which have also been discussed in connection with the threshold ion spectra recorded via the $S_1 5^1$ state of the complex. For example, according to this model, fragmentation from the $S_1 5^1$ into the monomer final states $S_1\underline{30}^1$ (5.9%), $S_1\underline{30}^2$ (11.9%), $S_1\underline{30}^3$ (24.4%), and $S_1\underline{27}^1$ (11.7%) should have a total probability of over 50%. As has already been noted, particularly ionization transitions from overtones of mode ν_{30} with $\Delta\nu = 0$ would fit the difference band in Figure 10. The ν_{30} vibration is an out-of-plane mode, which from intuition should couple very effectively with the intermolecular vdW modes. For the decay of the $S_1 6^2$ state however, this model predicts that only the $S_1 6^1$ state is populated with significant probability (93%). Thus, although the half-collision model is a very crude model, not taking into account the sequential character of the IVR/VP process, it predicts the population of fragment states with overtones of mode ν_{30} excited after pumping the $S_1 5^1$ state of the complex. This is remarkable, since we believe that mode ν_{30} (and its overtones) is responsible for the unexpected contour of certain VP bands (see Figures 7 and 10).

There is one final point left, which needs to be discussed briefly. Why could Parmenter et al. not perceive all fragmentation channels, observed by MATI spectroscopy after the excitation of the $S_1 5^1$ state of the complex? The most likely explanation is that transitions from the VP-populated states $\underline{30}^1$, $\underline{30}^2$, $\underline{30}^3$, and $\underline{27}^1$ in the S_1 into vibrational states of the S_0 are covered by stronger bands due to transitions from the final states $S_1\underline{0}^0$ and $S_1\underline{6}^1$ of the fragment. Parmenter et al. quoted a resolution of about 12 cm^{-1} for their dispersed fluorescence spectra. The transitions $\underline{30}_1^1$ and $\underline{27}_1^1$ are shifted by -38 and -43 cm^{-1} relative to the $\underline{0}_0^0$ transition (a summary of the vibrational modes of *p*-DFB in the S_0, S_1, and the cationic state is given in ref 30). Thus, these transitions would be covered by the $\underline{6}_1^1$ band (-40 cm^{-1}). In addition, also unfavorable Franck−Condon factors could possibly result in poorly pronounced fluorescence bands.

5. Conclusion

In this work, we could give evidence that the predissociation of vdW complexes in vibronically excited intermediate states can be studied by means of the MATI spectroscopy. We could show that the vibrationally induced predissociation of a vibronically excited complex strongly depends on the initially excited vibration of the complex. Thus the MATI results basically corroborated the findings of Parmenter et al., which were obtained by means of UV fluorescence spectroscopy. Of particular interest was the observation of the fragmentation of the two quasi degenerated vibrational states $S_1 5^1$ and $S_1 6^2$ into the final states $S_1\underline{0}^0$ and $S_1\underline{6}^1$ of the monomer. Thus two final states, one with minimum and one with maximum translational energy imparted to the Ar atom, are the dominant exit channels. In contrast to the earlier findings of Parmenter et al., the threshold ion spectra recorded via the $S_1 5^1$ complex state gave evidence for additional fragmentation channels, which have not

been observed or assigned in the fluorescence spectra. The dominant one is the out of plane vibrational mode ν_{30} as well as its overtones, which should couple with the dissociation continuum very well. We also deduced larger dissociation energies for the complex in the S_0, S_1, and the ionic ground state, respectively. Thus we could demonstrate that the MATI spectroscopy is an complementary method to the fluorescence spectroscopy. Particularly by applying a pump−probe method with ultrashort laser pulses, the predissociation dynamics of weakly bound complexes could be studied in real time and state selectively.

References and Notes

(1) Butz, K. W.; Catlett, D. L., Jr.; Ewing, G. E.; Krajnovich, D.; Parmenter, C. S. *J. Phys. Chem.* **1986**, *90*, 3533.
(2) Jacobson, B. A.; Humphrey, S.; Rice, S. A. *J. Chem. Phys.* **1988**, 89, 5624.
(3) Müller-Dethlefs, K.; Sander, M.; Schlag, E. W. *Z. Naturforsch. Teil A* **1984**, *39*, 1089.
(4) Müller-Dethlefs, K.; Schlag, E. W. *Annu. Rev. Phys. Chem.* **1991**, *42*, 109.
(5) Zhu, L.; Johnson, P. M. *J. Chem. Phys.* **1991**, *94*, 5769.
(6) Brutschy, B. *Chem. Rev.* **1992**, *92*, 1567.
(7) Djafari, S.; Lembach, G.; Barth, H.-D.; Brutschy B. *Z. Phys. Chem.* **1996**, *195*, 253.
(8) Krause, H.; Neusser, H. J. *J. Chem. Phys.* **1992**, *97*, 5923.
(9) Krause, H.; Neusser, H. J. *J. Chem. Phys.* **1993**, *99*, 6278.
(10) Neusser, H, J.; Krause, H. *Chem. Rev.* **1994**, *94*, 1829.
(11) Grebner, Th. L.; Neusser, H. J. *Chem. Phys. Lett.* **1995**, *245*, 578.
(12) Lembach, G.; Brutschy, B. *Chem. Phys. Lett.* **1997**, *273*, 421.
(13) Lembach, G.; Brutschy, B. *J. Chem. Phys.* **1997**, *107*, 6156.
(14) Grebner, Th. L.; Unold, P. v.; Neusser, H. J. *J. Phys. Chem. A* **1997**, *101*, 158.
(15) Zhang, X.; Smith, J. M.; Knee, J. L. *J. Chem. Phys.* **1992**, *97*, 2843.
(16) Smith, J. M.; Zhang, X.; Knee, J. L. *J. Chem. Phys.* **1993,** *99*, 2550.
(17) Zhang, X.; Knee, J. L. *Faraday Discuss.* **1994**, *97*, 299.
(18) Smith, J. M.; Zhang, X.; Knee, J. L. *J. Phys. Chem.* **1995**, *99*, 1768.
(19) Alt, C. E.; Scherzer, W. G.; Selzle, H. L.; Schlag, E. W. *Chem. Phys. Lett*. **1994**, *224*, 366.
(20) Wilson, E. B., Jr. *Phys. Rev.* **1934**, *41*, 706.
(21) Mulliken, R. S. *J. Chem. Phys.* **1955**, *23*, 1997.
(22) Lembach, G.; Brutschy, B. *J. Phys. Chem.* **1996**, *100*, 19758.
(23) Robey, M. J.; Schlag, E. W. *J. Chem. Phys.* **1977**, *67*, 2775.
(24) Cvitaš, T.; Hollas, J. M. *Mol. Phys*. **1970**, *18*, 793.
(25) Coveleskie, R. A.; Parmenter, C. S. *J. Mol. Spectrosc*. **1981**, *86*, 86.
(26) Knight, A. E. W.; Kable, S. H. *J. Chem. Phys.* **1988**, *89*, 7139.
(27) Sekreta, E.; Viswanathan, K. S.; Reilly, J. P. *J. Chem. Phys.* **1989**, *90*, 5349.
(28) Fujii, M.; Kakinuma, T.; Mikami, N.; Ito, M. *Chem. Phys. Lett.* **1986**, *127*, 297.
(29) Rieger, D.; Reiser, G.; Müller-Dethlefs, K.; Schlag, E. W. *J. Phys. Chem.* **1992**, *96*, 12.
(30) Reiser, G.; Rieger, D.; Wright, T. G.; Müller-Dethlefs, K.; Schlag, E. W. *J. Phys. Chem.* **1993**, *97*, 4335.
(31) O, H.-K.; Parmenter, C. S.; Su, M.-C. *Ber. Bunsen-Ges. Phys. Chem.* **1988**, *92*, 253.
(32) Su, M.-C.; O, H.-K.; Parmenter, C. S. *Chem. Phys.* **1991**, *156*, 261.
(33) Guttman, C.; Rice, S. A. *J. Chem. Phys.* **1974**, *61*, 661.
(34) Sussmann, R.; Neusser, H. J. *J. Chem. Phys.* **1995**, *102*, 3055.
(35) Held, A.; Baranov, L. Ya.; Selzle, H. L.; Schlag, E. W. *J. Chem. Phys.* **1997**, *106*, 6848.
(36) Chupka, W. A. *J. Chem. Phys.* **1993**, *98*, 4520.
(37) Fujii, M.; Kakinuma, T.; Mikami, N.; Ito, M. *Chem. Phys. Lett.* **1986**, *127*, 297.
(38) Grebner, Th. L.; Unold, P. v.; Neusser, H. J. *J. Phys. Chem. A* **1997**, *101*, 158.
(39) Hobza, P.; Selzle H. L.; Schlag, E. W. *J. Chem. Phys.* **1993**, *99*, 2809.
(40) Sussmann, R.; Neuhauser, R.; Neusser, H. J. *Can. J. Phys.* **1994**, *72*, 2.
(41) Nimlos, M. R.; Young, A.; Bernstein, E. R.; Kelley, D. F. *J. Chem. Phys.* **1989**, *91*, 5268.
(42) Outhouse, E. A.; Bickel, G. A.; Demmer, D. R.; Wallace, S. C. *J. Chem. Phys.* **1991**, *95*, 6261.
(43) Parmenter, C. S.; Tang, K. Y. *Chem. Phys.* **1978**, *27*, 127.
(44) Catlett, D. L., Jr. Ph.D. Thesis, Indiana University, 1985. *To whom correspondence should be addressed.